Probabilistic Model of Neuronal Background Activity in Deep Brain Stimulation Trajectories

Eduard Bakstein[1(✉)], Tomas Sieger[1,2], Daniel Novak[1], and Robert Jech[2]

[1] Department of Cybernetics, Faculty of Electrical Engineering, Czech Technical University in Prague, Prague, Czech Republic
eduard.bakstein@fel.cvut.cz

[2] Department of Neurology and Center of Clinical Neuroscience, First Faculty of Medicine and General University Hospital, Charles University in Prague, 128 21 Prague, Czech Republic

Abstract. We present a probabilistic model for classification of micro-EEG signals, recorded during deep brain stimulation surgery for Parkinson's disease. The model uses parametric representation of neuronal background activity, estimated using normalized root-mean-square of the signal. Contrary to existing solutions using Bayes classifiers or Hidden Markov Models, our model uses smooth state-transitions represented by sigmoid functions, which ensures flexible model structure in combination with general optimizers for parameter estimation and model fitting. The presented model can easily be extended with additional parameters and constraints and is intended for fitting of a 3D anatomical model to micro-EEG data in further perspective. In an evaluation on 260 trajectories from 61 patients, the model showed classification accuracy 90.0 %, which was comparable to existing solutions. The evaluation proved the model successful in target identification and we conclude that its use for more complex tasks in the area of DBS planning and modeling is feasible.

Keywords: Deep brain stimulation · Microelectrode recordings · Probabilistic model

1 Introduction

The Deep Brain Stimulation (DBS), which consists of permanent electrical stimulation of the basal ganglia, has been used for treatment of Parkinson's disease (PD) and other movement disorders since the pioneering work by Benabid et al. in the early 1990s [4]. Since then, it has become a standard therapy for drug-resistant late-stage Parkinson's disease and is applied in hundreds of centers worldwide. In order to achieve a good clinical outcome, accurate positioning of the stimulation electrode is necessary. As the target structures are small — the most common target for PD, the subthalamic nucleus (STN) measures less than 10 mm along its largest dimension — and precision of imaging methods available prior to operation is relatively low ($\sim$ 1 mm voxel size in pre-operative magnetic

M.E. Renda et al. (Eds.): ITBAM 2016, LNCS 9832, pp. 97–111, 2016.
DOI: 10.1007/978-3-319-43949-5_7

resonance imaging scans), precise placement based solely on pre-operative imaging is hard.

To obtain a more accurate location information, a method called microrecording is employed in a vast majority of DBS centers [1]. In microrecording, a set of microelectrodes (tip diameter around 5 μm) is shifted through the brain and microelectrode EEG (also μEEG or MER) is recorded. The recorded signals are evaluated concurrently by a trained neurologist, who then identifies optimal position for the stimulation contacts. The evaluation is typically based on visual and auditory inspection of the signals, the main markers being neuronal firing pattern and especially amplitude of the neuronal background, which are higher in areas with higher neuron density — such as the STN. The accumulation of neurons in the STN is very high compared to the neighboring structure, which projects into the recorded signals as a sudden increase in the neuronal background activity as the electrode approaches the STN boundary, as well as appearance of rapidly spiking neurons once the electrode entered the nucleus. The former can be estimated by the root mean square (RMS) of the original signal [9,14], some authors also suggested signal with removed spikes or RMS of a band-pass filtered signal [10,11].

For a long time, efforts have been made to use machine learning models in place of the manual evaluation. This paper presents a probabilistic model of neuronal background activity along a microrecording trajectory, characterized by a normalized root-mean-square measure (NRMS). The suggested model is a logical extension of already existing models, which are summarized in the next section.

1.1 Existing Models

Early models used the neuronal background level, estimated using the normalized root-mean-square of the signal as an input to Bayesian classifier [9] or discrete hidden Markov model (HMM) [14]. These models included also the expected distance to target as an input, which utilizes the fact that the presurgical planning places the target (i.e. "depth 0") to a specific part of the STN. These models also used manual quantization or thresholding of the input parameters in order to achieve reasonably-sized discrete parametric space, that can be estimated from commonly-sized training datasets.

Extension to semi-markov models, including state duration (i.e. the length of nuclei pass) with continuous probability density function has been done by Taghva et al. [13], but has been evaluated only on simulated data. Other researchers investigated features such as high-frequency component of the neuronal background [10] or multiple features including power spectral density, firing rate and noise level coupled with a rule-based classifier composed of cascaded thresholds [5]. Support vector machine classifier on multiple signal features (RMS, nonlinear energy, curve length, zero crossings, standard deviation and

number of peaks) has been also implemented by Guillen et al. [7] with almost 100 % accuracy.[1]

The authors of [12] investigated the impact of recording length and density on performance of an HMM and concluded that precision of a previously published HMM model [14] was approximately half of the between-position distance.

1.2 Proposed Model

In this paper, we present a model based on the neuronal background level, which can be used as a basis for fitting anatomical 3D model directly to the recorded μEEG activity along parallel trajectories. The presented variant is a one-dimensional proof of concept, intended to verify the idea and compare its properties to existing well-performing models.

Similarly to the hidden semi-markov models used in [13], our model uses parametric representation of input feature space – the NRMS values computed according to [9] but without quantization. Contrary to HMM, our model uses smooth state to state transitions, motivated by properties of electrical field of the STN, observed on the training data.

A derived model, based on the proposed approach, can be used to introduce other requirements such as the expected length of STN pass for given trajectory, based on a-priori information from surgical planning. Owing to the smooth state transitions, the model has also a smooth likelihood function (and gradient) and can be fitted using general purpose optimization algorithms. Thanks to this property, the structure of the model is very flexible and can be easily modified and extended. Moreover, the model theoretically allows classification with accuracy beyond the resolution of the measured data. However, this may not be the case practically due to noise in the μEEG signal and other measurement inaccuracies.

2 Methods

The probabilistic model, presented in this paper, is based on the assumption of different distribution of neuronal background before, within and beyond the STN. Each of these distributions is represented parametrically and transitions between the consecutive distributions are modeled by the logistic sigmoid function (see Sect. 2.2 below). In this section, we give overview of the proposed model, as well as of the data collection and pre-processing.

2.1 Data Collection, Annotation and Pre-processing

The experimental dataset was collected during the standard surgical procedure of DBS implantation using a set of one to five tungsten microelectrodes, spaced

[1] The dataset in [7] consisted of 52 signals from four patients only and it is not clear whether the validation sample was completely independent in terms of similarity of neighbor segments — see e.g. [8] for description of a similar problem.

2 mm apart in a cross; the so-called Ben-gun configuration [6]. The microelectrode signals were recorded at each 5 mm along the trajectory using the Leadpoint recording system (Medtronic, MN), sampled at 24 kHz, band-pass filtered in the range 500–5000 Hz and stored for offline processing. Annotation of nucleus at each position was done manually by an expert neurologist [R.J.], based on visual and auditory inspection of the recorded signal.

To reduce the effect of motion-induced artifacts, we divided each signal into 1/3 s windows and selected the longest stationary component using the method presented in [3], which is an extension of method previously presented in [2]. Parameters of the method (detection threshold and window length) were selected in order to achieve best accuracy on a training database. This method was chosen in order to obtain at least some segment of each signal, even though it may contain electromagnetic and other interference, which would be marked as signal artifact by the stricter spectral method, presented in [3].

2.2 Electric Field of the STN

To obtain estimate of the neuronal background activity level, we calculated the root-mean-square (RMS) of the stationary portion of the signal. In accordance with [9], we computed the normalized RMS of the signal (NRMS) by dividing feature values of the whole trajectory by mean RMS values of the first 5 positions (which are assumed non-STN in a majority of recordings). Additionally, we normalized the 90th percentile of each NRMS trajectory to 3 in order to limit NRMS variability in the STN.

Observations of NRMS values before, within and after the STN confirmed different distribution in each part. After comparing likelihood of normal and log-normal distribution, we chose to model the NRMS values in each part by the best-fitting log-normal distribution.

Further explorative analysis was aimed at the shape of NRMS transition. Figure 1 presents NRMS training data, aligned around STN entry and exit, mean value for each distance to the transition and the sigmoid logistic function we chose to model the transition as a result.

2.3 Parametric Model of STN Background Activity

Model Structure. The proposed model of background activity along the DBS trajectory consists of probability density of the NRMS measure in the three different regions. These can be seen as continuous emission probabilities in three hidden states of an HMM. Contrary to an HMM, the proposed model uses no discrete state transitions that could be represented by a transition matrix, but uses smooth state transitions, represented by sigmoid (or logistic) functions. Due to that, standard evaluation methods used for HMM, such as the Viterbi algorithm, can not be used and are replaced by general constrained optimization.

The general idea of the proposed model is based on the following reasoning: one of the most obvious features, distinguishing DBS target structure in

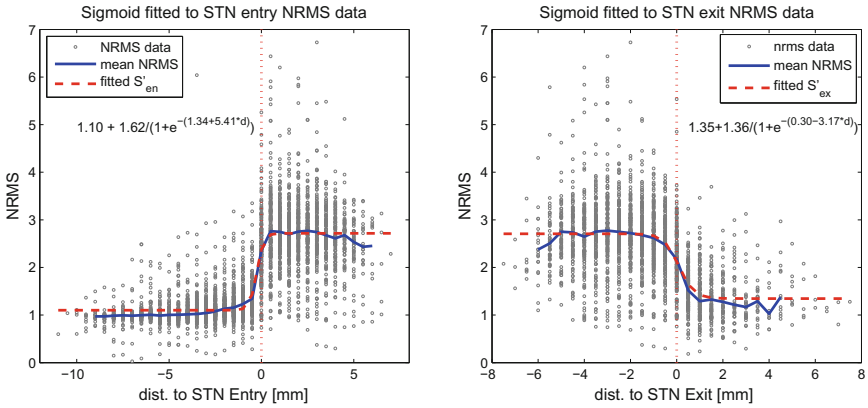

Fig. 1. NRMS values around STN entry and exit points (depth 0 on the x axis) from a set of training trajectories. The blue line represents mean NRMS value for each distance, the red dashed line shows fitted sigmoid functions S'_{en} and S'_{ex}, used to model STN entry and exit transitions, with parameters corresponding to the inlaid formula. (Color figure online)

the μEEG — in particular the STN — is signal power, represented here by signal NRMS. Based on our observations on training trajectories (see Sect. 2.2), as well as previous works (e.g. [10,11]), we assume different probability distribution of NRMS values in the areas before, within and beyond the STN and use the log-normal distribution as a model for the NRMS values in each area. Parameters of the log-normal model are estimated from labeled training data during the training phase.

In common settings, the μEEG signals are recorded at discrete depth steps (in our case every 0.5 mm). The task is therefore to classify signals, recorded at each position, to a correct class (i.e. identify the STN). We assume that the electrode can pass through the STN at most once and the trajectory can thus be divided into three consistent segments by two boundary points: STN entry and STN exit. In the evaluation phase we find optimal STN entry and exit points by maximizing the joint likelihood of the observed NRMS values along the trajectory with respect to the previously identified probability distributions. Simply put, the values before the assumed STN entry should be close to the expected value of the distribution before the STN, the values within the assumed STN should be close to the expected value of the distribution within STN and accordingly for the area beyond STN.

In order to increase theoretical precision of the model, as well as to improve its algebraic properties[2], we add smooth state transitions, modeled using logistic sigmoid functions. This approach also seems to be well in alignment with the observed statistical properties of NRMS values around STN boundary points — as can be

[2] Smooth state transitions using logistic sigmoid functions lead to smooth gradient and the resulting model is therefore easier to optimize.

seen in Fig. 1. The result of this addition is that rather than belonging to one particular state, each data point along the trajectory is assumed to be a partial member of all three states. Membership coefficients c_{pre}, c_{STN} and c_{post} of this combination are given by the sigmoid functions and depend on distance of given point from STN entry and exit. Illustration of the weighting can be found in Fig. 2.

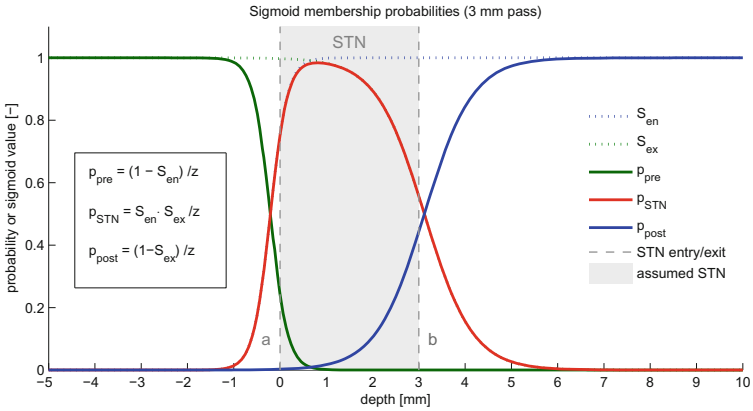

Fig. 2. Illustration of sigmoid transition functions S_{en} and S_{ex} and their application to the joint likelihood function from Eq. 8: each observed data point is assumed to be a partial member of all three hidden states. Probability density functions corresponding to each state are weighted using the membership probabilities $p_{pre}(i) = p(d_i \in pre|a, b, \boldsymbol{\Theta})$, $p_{STN}(i) = p(d_i \in STN|a, b, \boldsymbol{\Theta})$ and $p_{post}(i) = p(d_i \in post|a, b, \boldsymbol{\Theta})$ which are dependent on distance from the hypothetical STN entry and exit points a and b. The $z(i) = z_i$ is normalization coefficient - see Eqs. 10 and 13 for details.

In this paper, we present two variants of the model: (i) the basic *flex1*, based solely on the NRMS measure and (ii) extended model *flex2*, which adds a-priori distribution of expected STN entry and exit depths. The following sections provide formal definition of the model, as well as the training and evaluation procedure.

Training Phase. Supervised model training is performed on NRMS feature values $x_i \in \{x_1, x_2, ..., x_N\}$, extracted from MER data recorded at N recording positions at depths $d_i \in \{d_1, d_2, ..., d_N\}$. Manual expert annotation is provided for each recording position, labeling the signal as either *stn* or *other*. STN entry position i_{en} and exit depth i_{ex} is defined as index of the first and last occurence of *stn* label from the start of the trajectory. Trajectory is then divided into three parts; (i) before the STN with indices $I_{pre} = \langle 1, i_{en} - 1\rangle$, (ii) within the STN $I_{stn} = \langle i_{en}, i_{ex}\rangle$ and (iii) after the STN $I_{post} = \langle i_{ex} + 1, N\rangle$. Two groups of parameters are fitted during the training phase:

(i) Parameters of the log-normal probability distribution of NRMS feature values before the STN ($\boldsymbol{\theta}_{pre} = \{\hat{\sigma}_{pre}, \hat{\mu}_{pre}\}$), within the STN ($\boldsymbol{\theta}_{stn}$) and after

the STN ($\boldsymbol{\theta}_{post}$), where $\hat{\mu}$ and $\hat{\sigma}$ are maximum-likelihood estimates of location and scale parameters of the respective log-normal distribution, computed in standard way according to

$$\hat{\mu}_{pre} = \frac{\sum_{i \in I_{pre}} \ln(x_i)}{n_{pre}} \tag{1}$$

$$\hat{\sigma}_{pre} = \sqrt{\frac{\sum_{i \in I_{pre}} \left(\ln(x_i) - \hat{\mu}_{pre}\right)^2}{n_{pre}}} \tag{2}$$

where $n_{pre} = |I_{pre}|$, i.e. the number of positions with given label. Parameters for *stn* and *post* labels are computed accordingly on samples from the I_{stn} and I_{post} sets.

(ii) Parameters defining the shape of the sigmoid transition functions at STN entry (β^0_{en} and β^1_{en}) and exit (β^0_{ex} and β^1_{ex}). Here, the parameter β^0 represents shift and β^1 steepness of the respective logistic sigmoid function, defined as

$$S'_{en}(d_i) = \alpha^0_{en} + \alpha^1_{en} \cdot \left(1 + \exp -(\beta^0_{en} + \beta^1_{en}(d_i - d_{en}))\right)^{-1} \tag{3}$$

for STN entry and

$$S'_{ex}(d_i) = \alpha^0_{ex} + \alpha^1_{ex} \cdot \left(1 + \exp -(\beta^0_{ex} + \beta^1_{ex}(d_i - d_{ex}))\right)^{-1} \tag{4}$$

for STN exit, where d_{en} is STN entry depth and d_{ex} STN exit depth. The additional parameters α^0 (shift along the y axis) and α^1 (scaling factor) serve to provide sufficient degrees of freedom to achieve appropriate fit. However, these parameters are not part of the model and are not stored as both are replaced by the log-normal probability density functions modeling the NRMS values in the respective area. Note that contrary to shifted and scaled functions S'_{en} and S'_{ex} fitted during the training phase, standard logistic functions S_{en} and S_{ex} from Eqs. 11 and 12 are used during evaluation.
Fitting can be done using general purpose optimization function minimizing mean square error on all training data at once, according to:

$$\underset{\alpha^0_{en},\alpha^1_{en},\beta^0_{en},\beta^1_{en}}{arg\,\min} \sum_{i \in I_{pre}, I_{stn}} \left(S'_{en}(d_i, \alpha^0_{en}, \alpha^1_{en}, \beta^0_{en}, \beta^1_{en}) - x_i\right)^2 \tag{5}$$

and similarly for S'_{ex}. Only data labeled as *pre* and *stn* are used to fit parameters of S'_{en} and data labeled as *stn* and *post* are used to fit S'_{ex}. Initial parameters are set to $\left[\alpha^0_{en}, \alpha^1_{en}, \beta^0_{en}, \beta^1_{en}\right] = [1, 1, 0, 1]$ and $\left[\alpha^0_{ex}, \alpha^1_{ex}, \beta^0_{ex}, \beta^1_{ex}\right] = [1, 1, 0, -1]$

The trained model is then completely characterized by parameter vector $\boldsymbol{\Theta} = \{\boldsymbol{\theta}_{pre}, \boldsymbol{\theta}_{stn}, \boldsymbol{\theta}_{post}, \beta^0_{en}, \beta^1_{en}, \beta^0_{ex}, \beta^1_{ex}\}$, encompassing both log-normal emission probabilities and steepness and shift parameters of the sigmoid transition functions. If more trajectories are available for training, both parameter groups are estimated using all training data at once, given that appropriate labels and STN entry and exit depths are applied for each trajectory separately.

Extended Model. The presented model structure uses no prior information about expected STN entry and exit depths. It is possible to modify the model by adding empirical distribution of entry and exit depths, modeled using the normal distribution $p_a = N(\mu_a, \sigma_a)$ and $p_b = N(\mu_b, \sigma_b)$. The parameters can be estimated using the standard maximum likelihood estimates of mean and standard deviation. This will lead to addition of four parameters. We will denote the extended parameter vector $\boldsymbol{\Theta}'$, the extended model is then nicknamed *flex2* in the results section.

Model Evaluation. In the evaluation step, the model with parameters $\boldsymbol{\Theta}$ is fitted to a trajectory formed by a sequence of feature values x_i measured at corresponding depths d_i. Optimal posterior STN entry and exit points a and b are identified by minimizing the negative log-likelihood function

$$\{a, b\} = \underset{a,b}{arg\,\min} \sum_{i=1}^{N} -\ln(L(\{x_i, d_i\}|a, b, \boldsymbol{\Theta})) \tag{6}$$

The joint likelihood for position i at fixed values of STN entry and exit depths a and b and all three possible states (*pre*, *STN* and *post*) is given by:

$$\begin{aligned} L(\{x_i, d_i\}|a, b, \boldsymbol{\Theta}) &= p(\{x_i, d_i\}|a, b, \boldsymbol{\Theta}) \\ &= p(x_i, d_i \in pre|a, b, \boldsymbol{\Theta}) \\ &\quad + p(x_i, d_i \in STN|a, b, \boldsymbol{\Theta}) \\ &\quad + p(x_i, d_i \in post|a, b, \boldsymbol{\Theta}) \end{aligned} \tag{7}$$

By expanding the probabilities in Eq. 7 using the Bayes' theorem, we get

$$\begin{aligned} L(\{x_i, d_i\}|a, b, \boldsymbol{\Theta}) &= p(x_i|d_i \in pre, \boldsymbol{\Theta}) \cdot p(d_i \in pre|a, b, \boldsymbol{\Theta}) \\ &\quad + p(x_i|d_i \in STN, \boldsymbol{\Theta}) \cdot p(d_i \in STN|a, b, \boldsymbol{\Theta}) \\ &\quad + p(x_i|d_i \in post, \boldsymbol{\Theta}) \cdot p(d_i \in post|a, b, \boldsymbol{\Theta}) \end{aligned} \tag{8}$$

where the probability $p(x_i|d_i \in pre, \boldsymbol{\Theta})$ represents the emission probability in state *pre* and is computed using the standard probability density function of the log-normal distribution in the area before STN:

$$p(x_i, pre|\boldsymbol{\Theta}) = \frac{1}{x_i \hat{\sigma}_{pre}\sqrt{2\pi}} \quad \exp - \frac{(\ln(x_i) - \hat{\mu}_{pre})^2}{2\hat{\sigma}_{pre}^2}, \tag{9}$$

using parameters of the log-normal distribution $\hat{\mu}_{pre}$ and $\hat{\sigma}_{pre}$, obtained in the training phase according to Eqs. 1 and 2 respectively. The probabilities $p(x_i|STN, \boldsymbol{\Theta})$ and $p(x_i|post, \boldsymbol{\Theta})$ for NRMS distribution inside and beyond the STN are computed accordingly. The class membership probabilities $p(pre|a, b, \boldsymbol{\Theta})$ from Eq. 8 (similarly for states *STN* and *post*) depend on the distance between depth d_i and currently assumed STN borders a and b and are computed from the sigmoid transition functions as follows:

$$\begin{aligned} p(d_i \in pre|a,b,\boldsymbol{\Theta}) &= (1 - S_{en}(d_i,a|\boldsymbol{\Theta}))/z_i \\ p(d_i \in STN|a,b,\boldsymbol{\Theta}) &= S_{en}(d_i,a|\boldsymbol{\Theta}) \cdot S_{ex}(d_i,b|\boldsymbol{\Theta})/z_i \\ p(d_i \in post|a,b,\boldsymbol{\Theta}) &= (1 - S_{ex}(d_i,b|\boldsymbol{\Theta}))/z_i \end{aligned} \tag{10}$$

using the sigmoid transition functions S_{en} and S_{ex}:

$$S_{en}(d_i) = \left(1 + \exp -(\beta^0_{en} + \beta^1_{en}(a - d_i))\right)^{-1} \tag{11}$$

for STN entry and equivalently

$$S_{ex}(d_i) = \left(1 + \exp -(\beta^0_{ex} + \beta^1_{ex}(b - d_i))\right)^{-1} \tag{12}$$

for STN exit. The z_i in Eq. 10 is a normalization coefficient ensuring that the class membership probabilities add to one under all circumstances[3]:

$$z_i = (1 - S_{en}(d_i,a|\boldsymbol{\Theta})) + S_{en}(d_i,a|\boldsymbol{\Theta}) \cdot S_{ex}(d_i,b|\boldsymbol{\Theta}) + (1 - S_{ex}(d_i,b|\boldsymbol{\Theta})). \tag{13}$$

In case of the extended model *flex2*, the minimization will take the following form:

$$\{a,b\} = \underset{a,b}{arg\,min} \left[\sum_{i=1}^{N} (-\ln(L(d_i,a,b|\boldsymbol{\Theta})) - \lambda ln(p_a(a|\boldsymbol{\Theta'}) \cdot p_b(b|\boldsymbol{\Theta'})))\right] \tag{14}$$

where the summation $L(x_i,a,b|\boldsymbol{\Theta})$ is the same as in Eq. (6) and the new $p_a(a|\boldsymbol{\Theta'})$ and $p_b(b|\boldsymbol{\Theta'})$ are probabilities of STN entry at depth a and exit at depth b, computed from the normal probability density function

$$p_a(a|\boldsymbol{\Theta'}) = \frac{1}{\sigma_a\sqrt{2\pi}} \quad \exp -\frac{(a - \mu_a)^2}{2\sigma_a^2} \tag{15}$$

and represent the probability of STN entry at depth a and exit at depth b. The parameter λ can be used to assign more/less importance to the a-priori depth distribution, compared to the observation-based likelihood element. In case of the presented results, we set the value of $\lambda = 1.75$ which optimized train-set accuracy.

As this process can be vectorized and the parametric space is only two-dimensional and bounded, standard optimization algorithms with empirical gradient can be used to search for optimal parameters. In our case, we used constrained optimization with conditions requiring that $a \leq b$ (the entry depth a is lower or equal to exit depth b), $a \geq d_1$ and $b \leq d_N$ (entry and exit depths must be in the range of the data).

The parametric space may contain local optima (depending on the shape of NRMS values along given trajectory) and it is therefore very useful to provide

[3] Value of this normalization coefficient will however be close to one in most circumstances and reaches around 1.2 in the extreme case when $a = b$ using sigmoid parameters from Fig. 1.

reasonable initialization of a and b. In our implementation, the initialization was set as the mean entry and exit depths from the training data: μ_a and μ_b[4]. Note that both a and b are real numbers and are not restricted to the set of actually measured depths.

2.4 Crossvalidation

To evaluate the proposed model on real data and compare its classification ability against existing models, we evaluated the model in a 20-fold crossvalidation: in each fold, 5 % of available trajectories were left out for validation, while the remaining data were used for estimation of model parameters. This lead to 20 sets of error measures for each classifier which were than averaged to obtain final estimates. Larger number of crossvalidation folds was chosen in order to obtain better estimate of error variability on different validation datasets.

The models compared were (i) Bayes classifier from [9] based on discrete joint probability distribution of NRMS and depth and an (ii) HMM model, based on the same discrete probability distribution (used as emission probabilities), with transition probabilities estimated from the training data in a standard way and two variants of the proposed model: (iii) *flex1*, based solely on NRMS and (iv) *flex2* with distribution of entry and exit depths.

3 Experimental Results

3.1 Data Summary

In total, we collected 6576 signals from 260 electrode passes in 117 DBS trajectories in 61 patients. Length of recorded signals was 10 s. After discarding non-stationary signal segments, the mean length of raw signal segment that entered the NRMS calculation was 8.76 s (median 9.67 s). In each crossvalidation fold, 13 electrode passes were used for validation, while the remaining 247 were used for training.

3.2 Classification Results and Discussion

Mean values of classification sensitivity, specificity and accuracy are presented in Table 1, while distribution of these error measures on the 20 validation sets can be found in Fig. 3. Even though the results of all methods were very similar (as can be seen especially in Fig. 3), the highest mean test accuracy was achieved by the *hmm* model – 90.2 %, closely followed by the *flex2* model with 90.0 %. Both models were also best in terms of specificity, while the best validation set sensitivity was achieved by the *hmm* and *bayes* classifiers.

Comparing two variants of the proposed method, the *flex2* model with entry depth distribution achieved better results than the NRMS-only variant *flex1*. The latter model tended to converge to local optima on trajectories with high noise level or non-standard NRMS shape.

[4] In the case with no entry/exit depth distribution, the initial parameters were set as the middle of the trajectory for a and the 3/4 of the trajectory for b.

Table 1. Classification results (error measures from the 20-fold crossvalidation) comparing the results of Bayes classifier [9] (*bayes*), Hidden Markov model (*hmm*), suggested model based solely on the NRMS (*flex1*) and extended model with distribution of STN entry and exit depth (*flex2*). See also Fig. 3.

	Train			Test		
	Accuracy	Sensitivity	Specificity	Accuracy	Sensitivity	Specificity
bayes	90.4	84.1	94.1	89.0	82.5	92.8
hmm	91.3	83.8	95.7	90.2	83.1	94.3
flex1	88.5	80.9	92.9	88.0	80.6	92.2
flex2	90.1	83.2	94.1	90.0	83.1	94.1

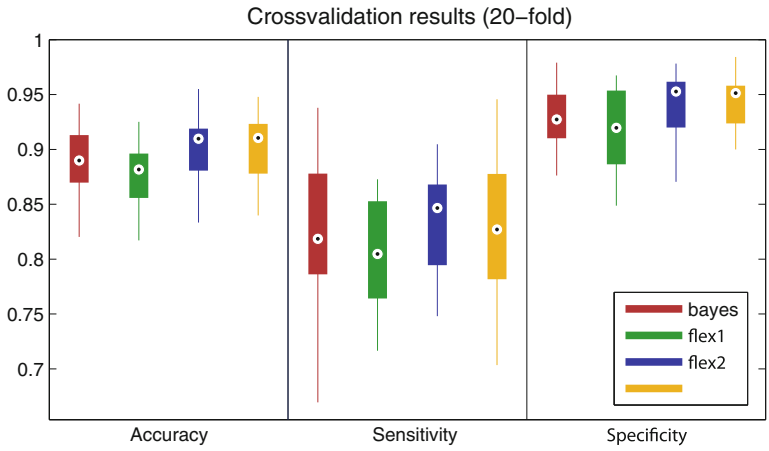

Fig. 3. Classification results on the 20 validation sets: *bayes* classifier [9], Hidden Markov model (*hmm*), suggested model, based exclusively on NRMS (*flex1*) and extended model with added a-priori entry and exit depth distribution (*flex2*).

3.3 Fitting of Individual Trajectories and Log-Likelihood Function Shape

Apart from the overall results, we also evaluated results on individual trajectories. The *bayes* model, which from definition put no constraints on the resulting label vector, was capable of classifying non-consecutive trajectories (interrupted STN labels) — this may have lead to the rather high sensitivity on the training data. As for the proposed models, the *flex1* NRMS-only variant tended to fit zero-length STN near the end of the trajectory in cases of non-standard STN passes where the NRMS did not exhibit the standard low–high–low profile or contained strong local peaks. The addition of entry and exit depth distribution in the *flex2* model variant reduced this problem and lead to improved classification accuracy.

An example of a successful STN classification on a typical trajectory using the *flex1* model can be seen in Fig. 4, while the corresponding negative log-likelihood function from Eq. 8 can be seen in Fig. 5. Note that the log-likelihood function is defined only for $a \leq b$. In the case of the *flex2* model, the values of the likelihood function around the a-priori expected entry and exit depth are further reduced by the additional component in Eq. 14, which increases the performance especially in cases with high noise in NRMS values.

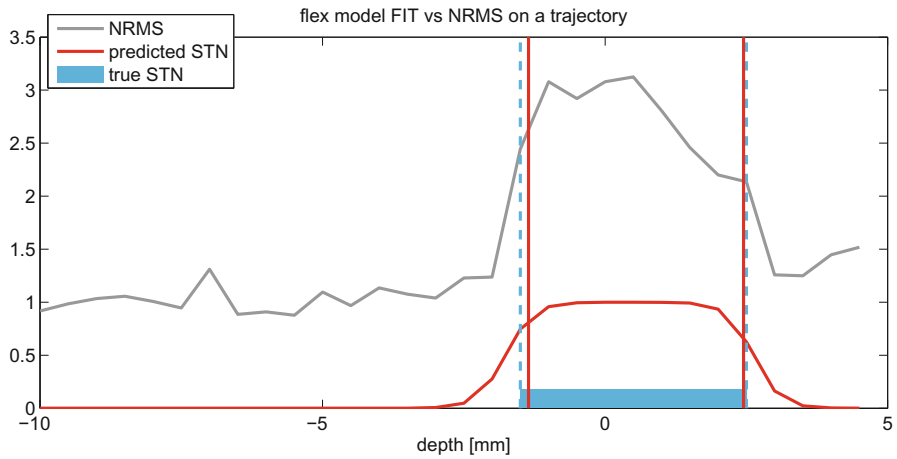

Fig. 4. Example of *flex1* model fit (red vertical lines — estimated position, red curve — sigmoid weighting function) to a NRMS recorded along a trajectory (grey). The expert-labeled STN position is shown in blue. (Color figure online)

4 Discussion and Further Work

The presented model achieved comparable accuracy to existing approaches, represented by bayesian classifiers [9] and HMM [14]. The results of HMM and hidden semi-markov models, presented by Taghva et al. [13] were much superior, but were evaluated on simulated data only. In summary, the presented extended model (*flex2*) achieved mean classification accuracy 90.0 %, sensitivity 83.1 % and specificity 94.1 % on the test set. As seen from the heavy overlap of different method's results, clearly visible in Fig. 3, we can conclude that it is rather robustness of the NRMS feature itself than the model structure, that has major impact on the results.

The main aim of this paper was to prove feasibility and efficacy of a probabilistic model which is variable in structure and can potentially be used for fitting of an anatomical 3D model to μEEG signals in multi-electrode setting. In such case, the inside and outside volume of the anatomical model would yield different emission probability distribution and further constraints or penalization

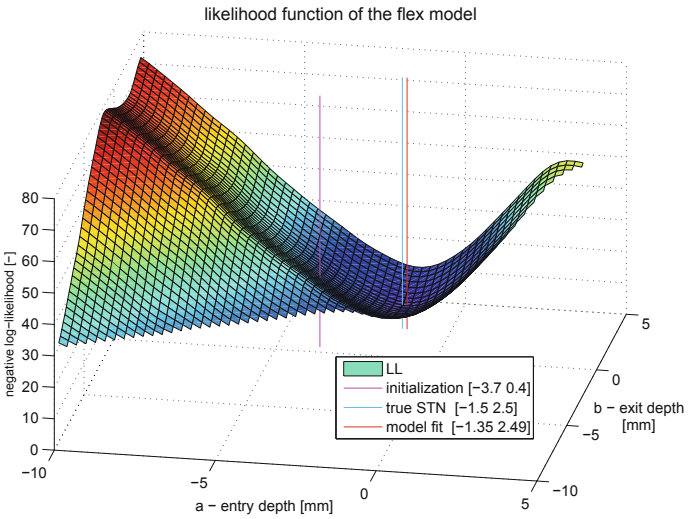

Fig. 5. Negative log-likelihood function of the *flex1* model shown as a function of hypothetical STN entry (a) and exit (b) depth. The vertical lines show initialization (magenta), model fit (red) and expert labels (blue). (Color figure online)

on model shift, scaling or rotation could be added easily into the minimization function. We have shown, that such addition of further constituents — such as the entry and exit depth in case of the *flex2* model — can be done and can contribute to improved classification accuracy.

The key part of the presented model is the use of smooth state transition functions, which ensure smooth shape of the resulting likelihood function and enable the use of general-purpose optimization techniques for model fitting. Another consequence of the use of sigmoid transition functions is that the detected transition point does not have to be truncated to a position of available measurement, but can be at an arbitrary position between states (i.e. the detected entry and exit depths are real numbers, not constrained by the depths where μEEG recordings are available).

The drawbacks of the presented model are that contrary to Bayes classifier or an HMM it is not straightforward to convert the presented method to an online algorithm, used e.g. during the surgery. Another weak point is the lack of closed-form solution to model evaluation and the necessity to use general optimization. Thanks to the low dimension[5] and small size of the parametric space, this does not pose a real problem in the presented settings, as the parameter estimation

[5] Dimension of the parametric space searched during the evaluation phase is two, due to two optimized parameters: STN entry a and exit b, both in the range of recorded depths. The search space is further reduced by the conditions defined at the end of Model Evaluation section, especially $a \leq b$.

took on average 0.9 s on the 247 training trajectories and model evaluation on all 260 trajectories took on average 4.5 s on a standard laptop PC.

Overall, the model provided good classification accuracy. In our further work, the model concept will be extended to fitting a 3D model to the μEEG trajectories, which may bring benefits to both surgical planning and modeling of neuronal activity within and around the STN.

Acknowledgement. The work presented in this paper has been supported by the students' grant agency of the CTU, no. SGS16/231/OHK3/3T/13, and by the Grant Agency of the Czech republic, grant no. 16-13323S.

References

1. Abosch, A., Timmermann, L., Bartley, S., Rietkerk, H.G., Whiting, D., Connolly, P.J., Lanctin, D., Hariz, M.I.: An international survey of deep brain stimulation procedural steps. Stereotact. Funct. Neurosurg. **91**(1), 1–11 (2013)
2. Aboy, M., Falkenberg, J.H.: An automatic algorithm for stationary segmentation of extracellular microelectrode recordings. Med. Biol. Eng. Comput. **44**(6), 511–515 (2006). http://www.ncbi.nlm.nih.gov/pubmed/16937202
3. Bakstein, E., Schneider, J., Sieger, T., Novak, D., Wild, J., Jech, R.: Supervised segmentation of microelectrode recording artifacts using power spectral density. In: 2015 37th Annual International Conference of the IEEE Engineering in Medicine and Biology Society (EMBC), vol. 2015-Novem, pp. 1524–1527. IEEE, August 2015. http://ieeexplore.ieee.org/lpdocs/epic03/wrapper.htm?arnumber=7318661
4. Benabid, A.L., Pollak, P., Gao, D., Hoffmann, D., Limousin, P., Gay, E., Payen, I., Benazzouz, A.: Chronic electrical stimulation of the ventralisintermedius nucleus of the thalamus as a treatment of movement disorders. J. Neurosurg. **84**(2), 203–214 (1996). http://dx.doi.org/10.3171/jns.1996.84.2.0203
5. Cagnan, H., Dolan, K., He, X., Contarino, M.F., Schuurman, R., van den Munckhof, P., Wadman, W.J., Bour, L., Martens, H.C.F.: Automatic subthalamic nucleus detection from microelectrode recordings based on noise level and neuronal activity. J. Neural. Eng. **8**(4), 46006 (2011). http://www.ncbi.nlm.nih.gov/pubmed/21628771, http://dx.doi.org/10.1088/1741-2560/8/4/046006
6. Gross, R.E., Krack, P., Rodriguez-Oroz, M.C., Rezai, A.R., Benabid, A.L.: Electrophysiological mapping for the implantation of deep brain stimulators for Parkinson's disease and tremor. Mov. Disord. **21**(Suppl. 1), S259–S283 (2006). http://dx.doi.org/10.1002/mds.20960
7. Guillen, P., Martinez-de Pison, F., Sanchez, R., Argaez, M., Velazquez, L.: Characterization of subcortical structures during deep brain stimulation utilizing support vector machines. In: 2011 Annual International Conference of the IEEE Engineering in Medicine and Biology Society, vol. 6, pp. 7949–7952. IEEE, August 2011. http://ieeexplore.ieee.org/xpls/absall.jsp?arnumber=6091960, http://ieeexplore.ieee.org/lpdocs/epic03/wrapper.htm?arnumber=6091960
8. Hammerla, N.Y., Plötz, T.: Let's (not) stick together: pairwise similarity biases cross-validation in activity recognition. In: Proceedings of the 2015 ACM International Joint Conference on Pervasive and Ubiquitous Computing, pp. 1041–1051 (2015)

9. Moran, A., Bar-Gad, I., Bergman, H., Israel, Z.: Real-time refinement of subthalamic nucleus targeting using Bayesian decision-making on the root meansquare measure. Mov. Disord. **21**(9), 1425–1431 (2006). http://www.ncbi.nlm.nih.gov/pubmed/16763982, http://dx.doi.org/10.1002/mds.20995
10. Novak, P., Daniluk, S., Ellias, S.A., Nazzaro, J.M.: Detection of the subthalamic nucleus in microelectrographic recordings in Parkinson disease using the high-frequency (> 500 hz) neuronal background. J. Neurosurg. **106**(1), 175–179 (2007). http://dx.doi.org/10.3171/jns.2007.106.1.175
11. Novak, P., Przybyszewski, A.W., Barborica, A., Ravin, P., Margolin, L., Pilitsis, J.G.: Localization of the subthalamic nucleus in Parkinson disease using multiunit activity. J. Neurol. Sci. **310**(1–2), 44–49 (2011). http://linkinghub.elsevier.com/retrieve/pii/S0022510X11004448
12. Shamir, R.R., Zaidel, A., Joskowicz, L., Bergman, H., Israel, Z.: Microelectrode recording duration and spatial density constraints for automatic targeting of the subthalamic nucleus. Stereotact. Funct. Neurosurg. **90**(5), 325–334 (2012). http://www.ncbi.nlm.nih.gov/pubmed/22854414, http://www.karger.com/doi/10.1159/000338252
13. Taghva, A.: Hidden Semi-Markov Models in the computerized decoding of microelectrode recording data for deep brain stimulator placement. World Neurosurg. **75**(5-6), 758–763.e4 (2011). http://www.ncbi.nlm.nih.gov/pubmed/21704949, http://linkinghub.elsevier.com/retrieve/pii/S187887501000848X
14. Zaidel, A., Spivak, A., Shpigelman, L., Bergman, H., Israel, Z.: Delimiting subterritories of the human subthalamic nucleus by means of microelectrode recordings and a Hidden Markov Model. Mov. Disord. **24**(12), 1785–1793 (2009). http://www.ncbi.nlm.nih.gov/pubmed/19533755, http://dx.doi.org/10.1002/mds.22674